Nuclear Instruments and Methods in Physics Research A325 (1993) 147–157
North-Holland

NUCLEAR INSTRUMENTS & METHODS IN PHYSICS RESEARCH
Section A

Temperature dependence of CsI(Tl) gamma-ray excited scintillation characteristics *

John D. Valentine [a], William W. Moses [b], Stephen E. Derenzo [b], David K. Wehe [a] and Glenn F. Knoll [a]

[a] *Department of Nuclear Engineering, The University of Michigan, Ann Arbor, MI 49109, USA*
[b] *Lawrence Berkeley Laboratory, University of California, Berkeley, CA 94720, USA*

Received 18 August 1992

The gamma-ray excited, temperature dependent scintillation characteristics of CsI(Tl) are reported over the temperature range of −100 to +50°C. The modified Bollinger–Thomas and shaped square wave methods were used to measure the rise and decay times. Emission spectra were measured using a monochromator and corrected for monochromator and photocathode spectral efficiencies. The shaped square wave method was also used to determine the scintillation yield as was a current mode method. The thermoluminescence emissions of CsI(Tl) were measured using the same current mode method. At room temperature, CsI(Tl) was found to have two primary decay components with decay time constants of $\tau_1 = 679 \pm 10$ ns (63.7%) and $\tau_2 = 3.34 \pm 0.14$ μs (36.1%), and to have emission bands at about 400 and 560 nm. The τ_1 luminescent state was observed to be populated by an exponential process with a resulting rise time constant of 19.6 ± 1.9 ns at room temperature. An ultra-fast decay component with a < 0.5 ns decay time was found to emit about 0.2% (about 100 photons/MeV) of the total scintillation light. Except for the ultra-fast decay time, the rise and decay time constants were observed to increase exponentially with inverse temperature. At −80°C τ_1 and τ_2 were determined to be 2.22 ± 0.33 μs and 18.0 ± 2.59 μs, respectively, while the 400 nm emission band was not observed below −50°C. At +50°C the decay constants were found to be 628 ns (70.5%) and 2.63 μs (29.3%) and both emission bands were present. The scintillation yield of CsI(Tl) was observed to be only slightly temperature dependent between −30 and +50°C, peaking at about −30°C (about 6% above the room temperature yield) and monotonically decreasing above and below this temperature. Four different commercially available CsI(Tl) crystals were used. Minimal variations in the measured scintillation characteristics were observed among these four crystals. Thermoluminescence emissions were observed to have peak yields at −90, −65, −40, +20, and possibly −55°C. The relative magnitudes and number of thermoluminescence peaks were found to vary from crystal to crystal.

1. Introduction

Gamma-ray detectors with high efficiency, low power consumption, low maintenance, and small size and weight have long been needed for many applications. While this ideal detector has not yet been achieved, the continuing development of solid-state photodiodes with large area and low noise has resulted in significant progress toward this realization. Silicon PIN photodiodes (PDs) have become one of the most commonly used photodetectors. Thallium-activated cesium iodide, CsI(Tl), is one scintillating crystal that has been widely used with these PDs. Although CsI(Tl) has been recognized as a scintillating crystal for several decades, its use has been limited due to the poor match of its emission spectrum with the radiant sensitivity of commercially available photocathodes. However, CsI(Tl) is the most luminous scintillating crystal known, having a measured absolute scintillation yield of 64 800 photons/MeV for gamma rays at room temperature [1]. CsI(Tl) scintillation light is very well matched with silicon PIN PDs, yielding a wavelength-averaged internal quantum efficiency of approximately 90% and an external quantum efficiency of about 70%; internal and external quantum efficiency are discussed by Geist et al. [2]. CsI(Tl) is also an efficient absorber of gamma rays, with a radiation length of 1.65 cm at 662 keV, a density of 4.51 g/cm^3, and an effective atomic number of 54. CsI(Tl) has a refractive index of 1.8 in the visible spectrum.

The temperature behavior of CsI(Tl) is of interest for two reasons. First, the thermally excited dark current present in silicon PIN PDs at room temperature

* This work was supported in part by the US Department of Energy under contracts no. DE-AC03-76SF00098 and DE-FG02-86NE37969, in part by Public Health Service Grants No. P01-25840 and No. R01-CA48002 and in part by a grant from the Whitaker Foundation.

Table 1
Published values of primary decay time constants at room temperature

Author(s)	τ_1 [ns]	τ_2 [μs]
Valentine et al. [18]	800	6.0
Pliavin [3]	800	1.6
Sastry and Thosar [4]	900	10
Managan [5]	550	0.7
Masunaga et al. [6]	800	1.2
Schotanus et al. [7]	600	3.4

limits the achievable energy resolution and suggests that low temperature operation might result in better energy resolution. Second, some applications require ambient temperatures other than typical room temperature. With this motivation, the temperature dependence of the scintillation characteristics of CsI(Tl) have been studied in the temperature range of −100 to +50°C.

The number of gamma-ray excited decay modes and their decay times for CsI(Tl) have been the subject of some controversy; both one and two primary decay modes have been reported. Table 1 shows some of the previously reported values of the two primary decay time constants of CsI(Tl), τ_1 and τ_2, at room temperature [3–7,18]. The confusion about the number of decay modes is due to the length and relatively small initial intensity of the longer component. However, the longer component is responsible for about 40% of the scintillation yield and leads to significant ballistic deficit when CsI(Tl) is used with commercially available linear amplifiers. The long decay component thus has a significant effect on pulse processing and the observed scintillation characteristics of CsI(Tl), e.g. energy resolution and light yield. Therefore, variations in the long decay time with temperature are of significant interest. The decay times of CsI(Tl) have been reported to be independent of thallium concentration for gamma-ray excitation [7]. This thallium concentration independence should result in small variation in decay times from crystal to crystal, independent of crystal origin.

For gamma-ray excitation at room temperature, the emission spectrum of CsI(Tl) has been reported to have up to four emission bands, the most prevalent of which peaks at about 560 nm [5–15]. The emission spectrum of a scintillating crystal is of interest for two reasons: the peak emission wavelengths yield information about the nature of the decay modes that govern the scintillation process, and knowledge of the spectral distribution allows the estimation of the effective quantum efficiency when used with a given photodetector. Measuring the absolute shape of the emission spectrum requires correcting recorded data for wavelength-dependent variations in monochromator efficiency and photocathode quantum efficiency. It is not stated in most cases whether the previously reported emission spectra have been corrected for such variations. We have corrected our data accordingly to yield an absolute emission spectrum shape.

The absolute scintillation yield is a dominant factor in determining the energy resolution of a scintillation detector because the yield governs pulse amplitude and the statistical fluctuations in the number of scintillation photons emitted. Since CsI(Tl) has the largest known scintillation yield, it has the potential for producing the best energy resolution of any scintillating crystal. The scintillation yield of CsI(Tl) is known to be dependent on thallium concentration, unlike the decay times [7]. Consequently, crystal-to-crystal variations of absolute scintillation yield are expected. This thallium concentration dependence may also manifest itself in differences in the temperature dependence of the scintillation yield.

CsI(Tl) is known to be thermoluminescent in the temperature range of interest [11,12]. For current mode and some pulse mode applications, the thermoluminescence can complicate data acquisition and analysis, and in some cases lead to erroneous results. Therefore, we have investigated the temperature ranges over which thermoluminescence occurs and whether these ranges vary from crystal to crystal.

Finally, CsI(Tl) crystals from several vendors were investigated to assess the differences in scintillation characteristics. Cubic crystals of 8 mm on a side were procured from Bicron Corporation, Horiba Crystal Products, Rexon Components, Inc., and Solon Technologies, Inc. The Solon Technologies, Inc. (STI) crystal was chosen at random to be used for the bulk of the measurements.

2. Theory

We shall assume that the luminescent states of CsI(Tl) are depopulated by exponential processes and are populated exponentially, instantaneously, or by a combination of both. With these assumptions, the temporal luminescence intensity of a scintillation event, $I(t)$, can be described by the sum of exponential components:

$$I(t) = \sum_j \frac{a_j}{\tau_j} e^{-t/\tau_j} = \sum_j I_j e^{-t/\tau_j} \qquad t \geq 0$$
$$I(t) = 0 \qquad t < 0, \tag{1}$$

where a_j, τ_j, and I_j are the integrated luminescence, characteristic time, and initial intensity of the jth exponential component. For all luminescent processes, the

characteristic time is a decay time constant and the integrated luminescence takes on a positive value, $a_{\text{decay}} > 0$. In the case of an exponential population of a luminescent state, an additional component in eq. (1) is necessary to describe the process. This rise component behaves as a negative integrated luminescence in the representation of eq. (1) ($a_{\text{rise}} < 0$), the characteristic time is a rise time constant, and the total integrated luminescence for the process is $a_{\text{rise}} + a_{\text{decay}}$. If a luminescent state is populated by a single exponential process then the absolute value of the initial intensities are equal, $I_{\text{decay}} = -I_{\text{rise}}$.

The relative luminescence intensity, $I(t)$, of CsI(Tl) was determined by the Bollinger–Thomas method [16], as modified by Moszynski and Bengtson [17], and by the shaped square wave (SSW) method [18]. The modified Bollinger–Thomas (MBT) method has become the industry standard for determining $I(t)$, and was thus used to both determine the most accurate estimates of the parameters and to confirm the applicability of determining $I(t)$ by the SSW method.

2.1. Modified Bollinger–Thomas method

The Bollinger–Thomas method was developed specifically for determining luminescence decay times. As modified, the method uses a trigger that is correlated in time with the initiation of the luminescence signal; a photodetector then randomly samples the luminescence distribution by restricting the mean number of photoelectrons generated per trigger to much less than one. This restriction is commonly realized by creating a "poor" crystal-to-photodetector geometry. To determine the true luminescence intensity $I(t)$, standard nuclear electronics, with an impulse response function $G(t)$, are used to acquire a timing spectrum. Consequently, the observed luminescence intensity $H(t)$ corresponds to the convolution of the impulse response function and the true luminescence intensity:

$$H(t) = \int_0^\infty I(t')G(t - t')\,\mathrm{d}t'. \tag{2}$$

For fitting purposes $I(t)$ was normalized to the total light yield, which is the sum of the a_j's. With this normalization, the a_j's represent the fraction of the total light emitted by jth process. For the case of an exponential process (a_{rise}, τ_{rise}) populating a luminescent state (a_{decay}, τ_{decay}), the fraction of the total light contributed by this rise/decay pair is $a_{\text{rise}} + a_{\text{decay}}$.

The measured data M_k are the number of counts in the kth bin corresponding to the time interval t_k to $t_k + \delta t$, and are analyzed using a nonlinear least squares fitting program. The fitted number of counts in the kth bin, F_k, is determined by summing the integral of the observed luminescence intensity and the chance coincidence rate, R_{ch}, contributions to that bin:

$$F_k = R_{\text{ch}}\delta t + \int_{t_k}^{t_k+\delta t} H(t)\,\mathrm{d}t. \tag{3}$$

The chance rate appears as a flat background on which the luminescence distribution is superimposed. Minimization of χ^2:

$$\chi^2 = \sum_k \frac{(M_k - F_k)^2}{\sigma_k^2} = \sum_k \frac{(M_k - F_k)^2}{F_k}, \tag{4}$$

results in the best estimates of the a_j and τ_j parameters, where F_k is the best estimate of the variance of the counts in the kth bin. The statistical uncertainties of the a_j's and τ_j's are determined by finding the largest and smallest value of each parameter on the surface defined by $\chi^2 + 1$ when all other parameters are free.

2.2. Shaped square wave method

The SSW method was developed specifically for the charge calibration of CsI(Tl)/photodiode systems to account for the ballistic deficit due to the long decay time constants. The SSW method relies on creating a calibration pulse of known charge with the same shape and amplitude as the full energy CsI(Tl) scintillation pulses such that both pulses experience the same ballistic deficit. When this is realized, the photopeak and calibration peak centroids will occur in the same channel of a multichannel analyzer, independent of amplifier shaping time. Creating a pulse of the same shape as the CsI(Tl) scintillation pulse is achieved by first splitting a square wave voltage pulse into a number of branches equal to the number of rise and decay times to be modeled. Each branch is then shaped with an RC circuit corresponding to a τ_j, inverted if the exponential component being modeled is a rise time, and attenuated to represent the appropriate a_j. Finally, the branches are summed forming the shaped square wave voltage pulse that is passed to the test capacitor of the charge sensitive preamplifier, where it is converted into a current pulse and processed in an identical manner to the scintillation pulse from the photodiode.

The RC time constants and attenuation factors were varied with potentiometers that were calibrated with an oscilloscope. The uncertainty of the calibration has been assumed to be dominated by the uncertainty in reading the oscilloscope and is estimated to be $\pm 5\%$ of the reported parameter value.

3. Scintillation decay time constants

The modified Bollinger–Thomas method used a barium fluoride (BaF_2) scintillating crystal coupled to a

Hamamatsu R-2059 PMT to provide a trigger. Another R-2059 PMT, 50 cm away from the CsI(Tl) crystal, provided the stop signal. The BaF_2 and CsI(Tl) were aligned with a 511 keV annihilation photon source between them to excite both crystals simultaneously. Timing signals were generated from the PMT outputs by a Tennelec TC-454 quad constant fraction discriminator. The time difference between the trigger and stop was then determined by a Tennelec TC-862 time-to-amplitude converter (TAC) and digitized by a LeCroy 3512 analog-to-digital converter. The CsI(Tl) crystals were placed in a separate, thermally-insulated, temperature-controlled enclosure that was optically coupled to the PMT via quartz lenses and air gaps. A brass block served as the heat sink and source for the enclosure. For low temperature operation, a constant flow of liquid nitrogen was passed through the block. The temperature regulation was provided by a computer-controlled heating element in the brass block (temperature regulation method A). The crystal temperature was monitored by placing a thermocouple in direct contact with the crystal.

The most reliable fitting results for the modified Bollinger–Thomas method are achieved with a TAC range $> 3\tau_j$ and a bin width $< 0.1\tau_j$. Since decay time constants as short as < 0.5 ns and as long as 18 μs were observed, these constraints would require taking data in 50 ps bins over a 50 μs range. The dynamic range of the TAC used was not large enough for this to be possible, thus data was acquired with two TAC ranges. Timing spectra were taken with a 1 μs TAC range at each temperature to accurately determine any exponential components with characteristic times of several hundred ns or less. For $T > -20$°C, data were also taken with a 20 μs TAC range in 16.64 ns bins, and for $T \leq -20$°C with a 50 μs range with 10.35 ns bins. These longer TAC ranges allowed the accurate determination of components with 1–20 μs characteristic times. The reported parameter values were determined through an iterative process of fitting the long and short TAC range data. First, the longer TAC range data was fit by allowing all of the parameters to vary (an initial best estimate of the longer decay components). The resulting values were then used as starting values for the 1 μs TAC range data, but only the parameters associated with the "shorter" components, less than about one microsecond, were allowed to vary (an initial best estimate of the rise and shorter decay components). Subsequent estimates of the "longer" and "shorter" parameters were made using the previous best estimates of the short and long range TAC data, respectively, until both sets converged. In most cases only a few iterations were required. The fits resulted in typical χ^2 per degree of freedom values of 1.05 to 1.2 for both the long and short TAC range data.

Fig. 1 shows the timing spectra at room temperature for the STI crystal. Along with decay times τ_1 and τ_2, 772 ± 8 ns (61.1%) and 3.53 ± 0.10 μs (38.7%), respectively, an ultra-fast component and a 22.7 ± 1.0 ns rise time that populates τ_1 ($I_1 = -I_{rise}$) are observed. The ultra-fast component appears as the three high channels at the beginning of the 1 μs TAC range spectrum and is not observed in the 20 μs TAC range data due to its small fraction of the total luminescence yield and the large bin width. The ultra-fast component has a decay time < 0.5 ns (0.5 ns is the timing resolution of the system used and thus the minimum decay time that can be accurately determined) and yields about 0.2% of all of the photons (about 100 photons/MeV). The rise time of CsI(Tl) is believed to be the longest of any known scintillating crystal. Table 2 compares the a_j's and τ_j's for the four different crystals at room temperature and 0°C. For $T \leq -30$°C, additional decay components ($j = 4,5$) were observed and are believed to be

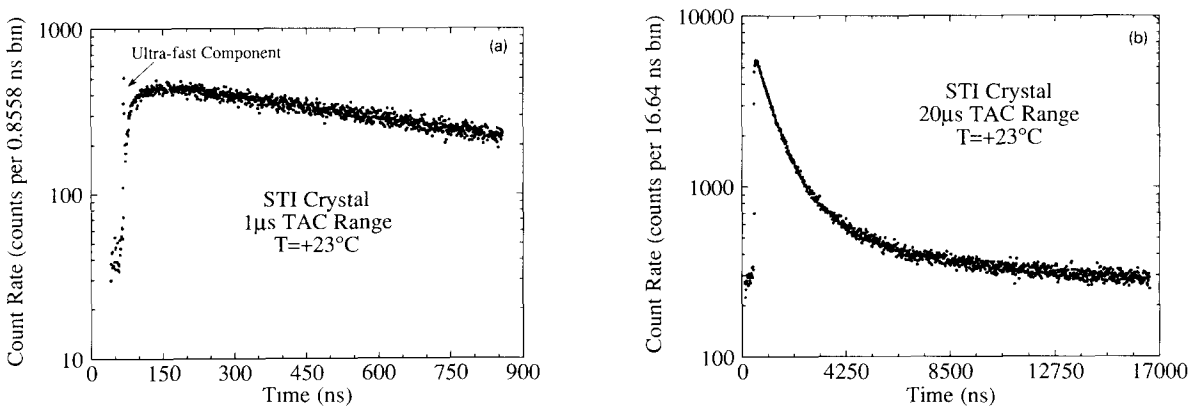

Fig. 1. Gamma-ray excited CsI(Tl) luminescence timing spectra at room temperature for the Solon Technologies, Inc. crystal.

Table 2
Comparison of rise and decay time constants for crystals from Solon Technologies, Inc., Bicron Corp., Horiba Crystal Products and Rexon Components, Inc. at room temperature and 0°C for the modified Bollinger–Thomas method

Crystal	Temperature [°C]	a_{rise}	τ_{rise} [ns]	a_1	τ_1 [ns]	a_2	τ_2 [μs]	$a_{ultra\text{-}fast}$	$\tau_{ultra\text{-}fast}$ [ns]
STI	+23	−0.016	22.7	0.627	772	0.387	3.53	0.002	< 0.5
Bicron		−0.021	28.3	0.659	677	0.361	3.36	0.001	< 0.5
Horiba		−0.018	19.6	0.655	679	0.361	3.34	0.002	< 0.5
Rexon		−0.020	23.7	0.635	646	0.383	3.25	0.003	< 0.5
STI	0	−0.026	36.8	0.610	784	0.413	4.31	0.002	< 0.5
Bicron		−0.023	38.0	0.619	837	0.402	4.21	0.001	< 0.5
Horiba		−0.021	30.4	0.625	778	0.394	4.36	0.002	< 0.5
Rexon		−0.026	33.6	0.621	753	0.403	3.88	0.003	< 0.5
Typical Uncertainty		±10%	±10%	±5%	±3%	±5%	±5%	±8%	

attributed to the luminescence of pure CsI. These decay components and the other fit results for all temperatures for the STI crystal are shown in table 3.

Even though the long decay component of CsI(Tl) yields 35–45% of the photons, its initial intensity, I_2, is about an order of magnitude lower than the main component, I_1. Accurately resolving τ_2 thus becomes strongly dependent on the knowledge of the flat background (chance coincidence rate). Since the initial intensity decreases with temperature while the background remains nearly constant, accurately determining the background becomes even more important with decreasing temperature.

Deich et al. [19,20] have observed the ultra-fast decay time and reported it to be ≤ 10 ps, independent of temperature over the range of 80–400 K, emitted with a broad emission band peaking at about 620 nm, and independent of crystal defects, impurities and activators. They have attributed this component to intraband luminescence induced when a "hot" charge carrier (an electron for gamma-ray excitation) liberates an inner valence band electron leaving a deep hole. As this deep hole moves toward the top of the valence band, it has a small probability of emitting a photon.

The rise time of CsI(Tl) became too long to accurately fit below −60°C. However, when the rise time was accurately fit, it was always observed to be associated with τ_1, as evidenced by the similarity of the initial intensities. Similarly, below −60°C the ability to accurately fit the long decay time is diminished because of signal-to-noise and the decay time approaching the limit of the TAC range. When the rise time or

Table 3
Rise and decay time constants for Solon Technologies, Inc. crystal as a function of temperature for the modified Bollinger–Thomas method

Temperature [°C]	a_{rise}	τ_{rise} [ns]	a_1	τ_1 [ns]	a_2	τ_2 [μs]	$a_{ultra\text{-}fast}$	$\tau_{ultra\text{-}fast}$ [ns]	a_4	τ_4 [ns]	a_5	τ_5 [ns]
+50	−0.012	13.3	0.717	628	0.293	2.63	0.002	< 0.5				
+40	−0.014	13.8	0.650	644	0.362	2.96	0.002	< 0.5				
+30	−0.014	13.5	0.656	635	0.356	3.12	0.002	< 0.5				
+20	−0.020	24.9	0.616	710	0.402	3.26	0.002	< 0.5				
+10	−0.019	25.5	0.611	749	0.406	3.85	0.003	< 0.5				
0	−0.026	36.8	0.610	784	0.413	4.31	0.002	< 0.5				
−10	−0.027	46.6	0.601	919	0.424	6.55	0.002	< 0.5				
−20	−0.034	60.7	0.599	989	0.432	7.77	0.003	< 0.5				
−30	−0.060	125	0.620	1100	0.406	8.76	0.002	< 0.5	0.001	1.81		
−40	−0.112	278	0.641	1310	0.467	11.3	0.002	< 0.5	0.001	3.23		
−50	−0.173	480	0.800	1760	0.370	11.8	0.002	< 0.5	0.003	4.91		
−60	−0.129	886	0.679	3040	0.443	13.4	0.003	< 0.5	0.004	7.94		
−80			0.171	2220	0.782	18.0	0.012	< 0.5	0.036	39.5		
−100			0.480	3520			0.042	< 0.5	0.376	171	0.101	19.8
Typical uncertainty	±10%	±10%	±5%	±5%	±5%	±10%	±10%		±15%	±20%	±14%	±18%

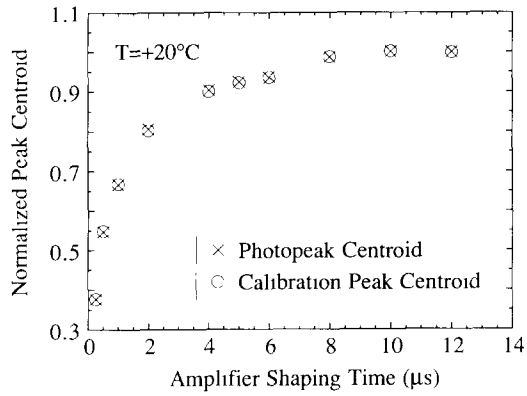

Fig. 2. Example of photopeak and calibration peak centroid matching by SSW method for Solon Technologies, Inc. crystal.

Table 4
Primary decay time constants and charge fraction ratios for the Solon Technologies, Inc crystal as a function of temperature for the SSW method, estimated uncertainty of ±5% on all values

Temperature [°C]	τ_1 [ns]	τ_2 [μs]	Q_2/Q_1
+30	809	5.00	0.680
+20	832	5.50	0.760
+10	956	6.85	0.742
0	1040	7.97	0.760
−10	1060	8.58	0.865
−20	1100	9.47	0.927
−30	1150	10.40	1.01
−40	1190	11.20	1.09
−50	1240	12.20	1.17
−60	1370	12.90	1.19

the long decay time become unresolvable, the a_j's no longer accurately estimate the fraction of the total light being emitted by jth process.

To determine τ_1 and τ_2 by the SSW method, the STI crystal was coupled to a Hamamatsu S3590-03 silicon PIN photodiode. A Canberra 2003BT charge sensitive preamplifier, a Canberra 2022 linear amplifier, and a multi-channel analyzer were used for pulse processing of the scintillation signal. To provide the necessary temperature control, the CsI(Tl) and PD were placed in a Tenney Jr. environmental chamber, modified for liquid nitrogen use. Pulse height spectra were taken at ten of the available amplifier shaping time constants (ranging from 0.25 to 12 μs) at 10°C increments over the −100 to +50°C temperature range with a 662 keV gamma-ray source. The SSW method was subsequently performed. An example of the matching of the photopeak and calibration peak centroids at each amplifier shaping time is shown in fig. 2. The SSW method is only sensitive to exponential components on the order of the amplifier shaping times and thus the rise time and ultra-fast decay time were not determined by this method. The ultra-fast decay was not observed because of its very small contribution to a single pulse, and the rise time was maintained at about 40 ns for the calibration at every temperature. Table 4 shows the SSW method results. Above +30°C, accurate estimates of the photopeak centroids at all amplifier shaping time constants were not achievable due to the photodiode noise. Below −60°C, τ_2 becomes longer than the longest amplifier shaping constant and the photopeak centroids for the shorter shaping times begin to become obscured by the noise shoulder. Consequently, for $T > +30$°C and $T < -60$°C the SSW method can not be used.

A comparison of the results from the modified Bollinger–Thomas method and SSW method is shown in fig. 3. Estimated uncertainties are, in most cases, smaller than the symbols used. The rise and decay

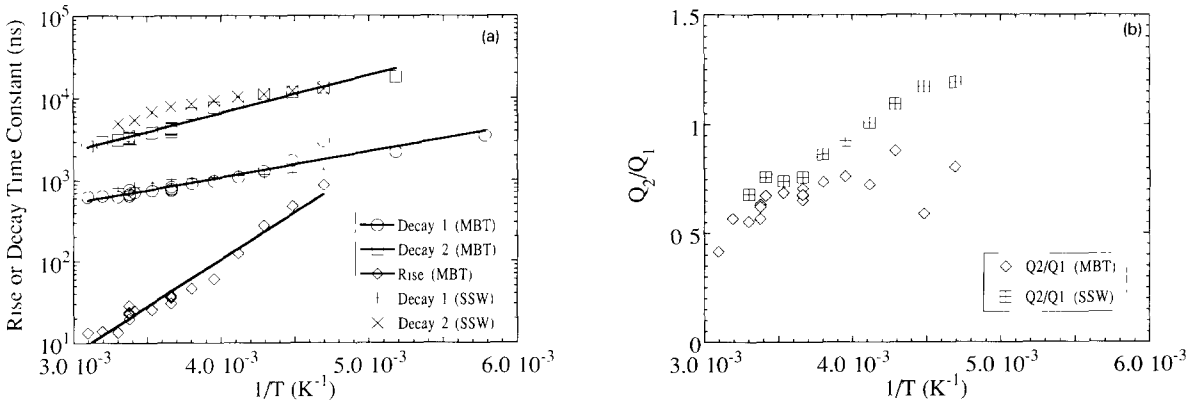

Fig. 3. (a) Rise and decay time results, and (b) charge contribution ratio results from modified Bollinger–Thomas (MBT) method and shaped square wave (SSW) method.

times are plotted versus $1/T$, since τ_j is expected to behave like:

$$\tau_j \propto e^{E_j/kT}, \quad (5)$$

where E_j is the activation energy of the jth process and k is the Boltzmann constant [21]. Activation energies of 0.23, 0.063, and 0.090 eV for the τ_{rise}, τ_1, and τ_2, respectively, were determined by fitting the modified Bollinger–Thomas results to eq. (5). The rise time activation energy, 0.23 eV, corresponds closely to the activation energy associated with the 90°-reorientation of V_k centers in CsI [22]. Consequently, the rise time has been attributed to the migration of V_k centers toward luminescence centers via 90°-reorientation. Although the SSW method yields some estimates of the primary decay time constants that are outside the uncertainties of the modified Bollinger–Thomas method results, the SSW method results are reasonable estimates with a possible systematic bias. The SSW method yields a ratio of charge contributions from the two primary components to the total pulse, Q_2/Q_1. This charge ratio is equivalent to the ratio of fractions, $a_2/(a_1 + a_{rise})$, from the modified Bollinger–Thomas method, as shown in fig. 3b. When the rise time can not be accurately fit, $T < -60$°C, the charge ratio can not be calculated. The systematic uncertainties in the SSW method results for the decay times and charge ratios are probably due to the rise time component not being modeled exactly at each temperature and inaccurate potentiometer calibration.

4. Emission spectrum

The emission spectra of the CsI(Tl) crystals were measured using a 0.125 m Jarrell–Ash MonoSpec 18 monochromator with two different 1200 line/mm gratings, one blazed for 300 nm and the other for 500 nm. The monochromator entrance and exit slits were 500 μm wide, which results in a 12 nm spectral resolution. 511 keV annihilation photons from a 0.7 mCi ^{68}Ge source were used to excite the crystals. The crystal of interest was placed at the focal point of a quartz lens; a similar lens then refocused the emissions onto the entrance slit of the monochromator. A Hamamatsu R-2059 PMT was placed at the exit slit of the monochromator in a thermally insulated enclosure. The PMT was cooled to −20°C to reduce the dark current, and a background rate of about 10 photoelectrons/s was thus achieved. The PMT was shielded from the source with lead bricks to prevent direct interactions of the 511 keV photons in the PMT. The output of the PMT was converted to a logic pulse by a Tennelec TC-454 constant fraction discriminator and subsequently counted with a Jorway 84 CAMAC scaler. The crystals and first focusing lens were placed in the same

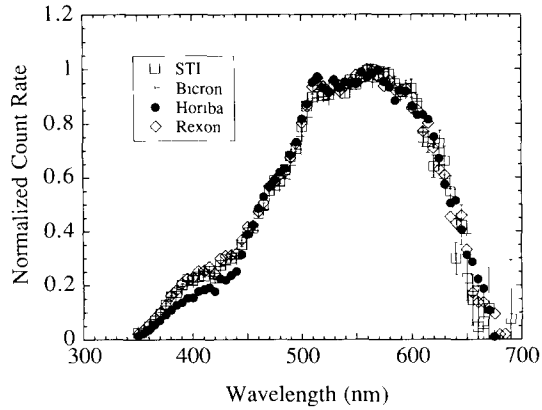

Fig. 4. Gamma-ray excited CsI(Tl) emission spectrum at room temperature for crystals from Bicron Corp., Horiba Crystal Products, Rexon Components, Inc., and Solon Technologies, Inc.

thermally insulated, temperature-controlled enclosure as was used for the modified Bollinger–Thomas method, and temperature regulation method A was used. The data were corrected for the spectral efficiency of the monochromator and PMT using a NIST traceable calibrated Hamamatsu L2196 Deuterium Lamp.

A comparison of the CsI(Tl) emission spectrum from the four different crystals at room temperature is shown in fig. 4 with the data normalized to unity at the peak emission count rate. The uncertainties shown in fig. 4 for the STI crystal are due to counting statistics only and are typical of the other emission spectra reported. Emission bands at about 400 and 560 nm are present and have been attributed to F-centers created by I^- vacancies and thallium luminescence centers, respectively [7]. Fig. 5 shows the emission spectrum for the STI crystal as a function of temperature, normal-

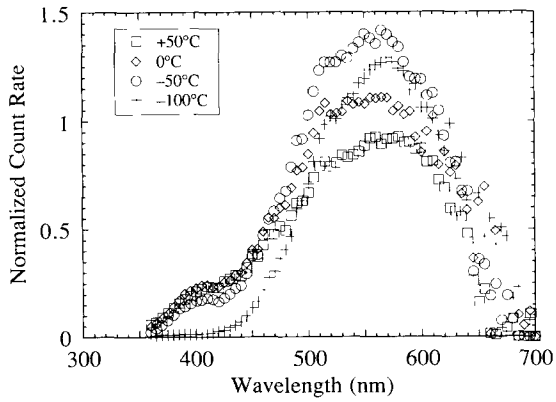

Fig. 5. Temperature dependence of gamma-ray excited CsI(Tl) emission spectrum for Solon Technologies, Inc. crystal.

ized to the peak emission count rate at room temperature. The emission spectrum appears to peak between 560 and 570 nm at all temperatures. The 400 nm band is observed to disappear between −50 and −75°C. This is believed to be due to the decreased mobility and thermal excitation of holes that recombine with the F-centers to create the 400 nm emission band. Although the 400 nm band is quite evident above −50°C, its relative contribution to a pulse is small. The small peak that appears in most of the emission spectra at about 520 nm is believed to be due to calibration inaccuracies and not a true emission peak. The change in relative peak count rate observed with changing temperature may be complicated by the CsI(Tl) thermoluminescence emissions, as will be discussed.

Spectrally resolved timing measurements were made to determine the temporal luminescence intensity of the 400 and 560 nm bands. By performing the modified Bollinger–Thomas method with the monochromator set at either 400 or 560 nm, $I(t)$ for those emission bands was measured. No significant deviation from the previously reported rise and decay time constants was observed for either emission band. Therefore, we conclude that the emission spectrum and temporal luminescence intensity of CsI(Tl) are independent.

5. Relative scintillation yield

Since the decay times of CsI(Tl) are temperature dependent, it is necessary to measure the scintillation yield using a method that either accounts for or is unaffected by changes in decay times. The SSW method is a pulse mode method that was developed for the purpose of determining scintillation yield by accounting for long decay times and changes in these decay times. A current mode method that is unaffected by decay time changes was also used. The current mode method was achieved by placing an active source near the CsI(Tl) crystal and measuring the PMT output current with an electrometer. It was assumed that the PMT output current is directly proportional to the scintillation yield. The crystal was placed in the same enclosure used for the emission spectrum and modified Bollinger–Thomas measurements. The crystal temperature was controlled by a slightly different method because thermoluminescence was observed to affect these measurements both while increasing temperature and at thermal equilibrium, as further discussed in the next section. To avoid these problems the crystal was initially heated to 50°C, the heating element turned off, and the crystal cooled at a rate of about 1°C per minute by manually regulating the liquid nitrogen flow such that the crystal temperature was monotonically decreased (temperature regulation method B). The light collection efficiency and photodetector quantum efficiency were assumed to be independent of CsI(Tl) crystal temperature for both methods.

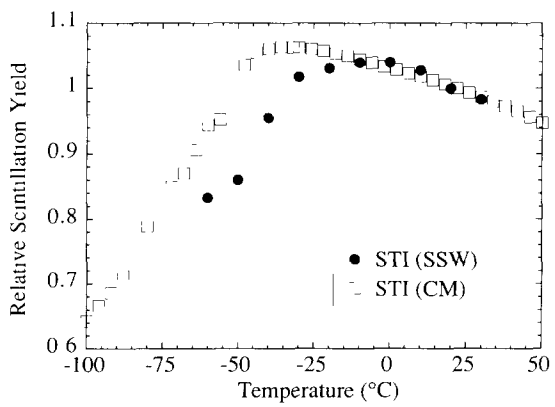

Fig. 6. Comparison of CsI(Tl) relative scintillation yield results from shaped square wave (SSW) method and current mode (CM) method for Solon Technologies, Inc. crystal

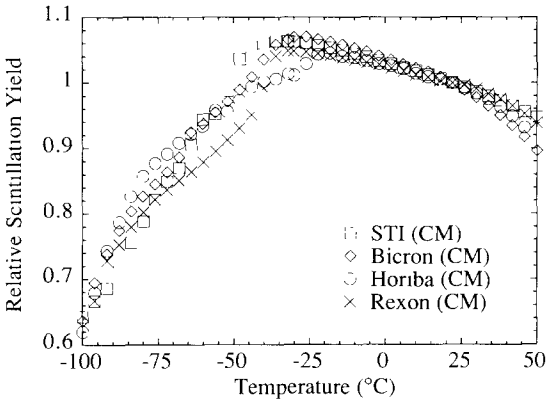

Fig. 7. CsI(Tl) relative scintillation yield results for crystals from Bicron Corp., Horiba Crystal Products, Rexon Components, Inc , and Solon Technologies, Inc. measured by current mode method.

A comparison of the results from the SSW method and current mode method is shown in fig. 6 for the STI crystal, while the results from the current mode method for all four crystals are shown in fig. 7. The relative yields have been normalized to unity at the room temperature yield. The scintillation yield is observed to be only slightly temperature dependent in the range of −30 to +50°C varying from about 5% above to 10% below the room temperature yield, respectively. The differences observed between the results for the SSW and current mode methods for the STI crystal are assumed to be due to not accounting for the temperature dependence of the photodiode quantum efficiency and not modeling the rise time exactly at each temperature in the SSW method. Thus, we believe that the

current mode method yields a more accurate estimate of the temperature dependence of the CsI(Tl) scintillation yield.

6. Thermoluminescence

The current mode scintillation yield measurements were initially made using temperature regulation method A. However, the scintillation yield for the STI crystal was observed to deviate by factors of up to four in the temperature range of −80 to −30°C when warming the crystal as opposed to cooling the crystal. This deviation has been attributed to thermoluminescence emission. Additionally, thermoluminescence was observed to affect the current mode method results at thermal equilibrium for temperature regulation method A in the same temperature range. Furthermore, thermoluminescence release was not observed to affect the current mode measurements when temperature regulation method B was used.

To determine the temperatures and magnitudes of the peak thermoluminescence emissions, the "glow curves" of each CsI(Tl) crystal were measured. After the crystals came to thermal equilibrium at −100°C, the liquid nitrogen flow was turned off and the heating element turned on. The crystal was subsequently heated at a rate of about 5°C per minute while the PMT output current was recorded. The crystal was continuously irradiated during the measurements, thus it was necessary to subtract the gamma-ray excited scintillation yield from the recorded data to arrive at thermoluminescence yield. The resulting "glow curves" for the four different crystals are shown in fig. 8. The thermoluminescence yield for each crystal has been normalized to its room temperature scintillation yield. It is

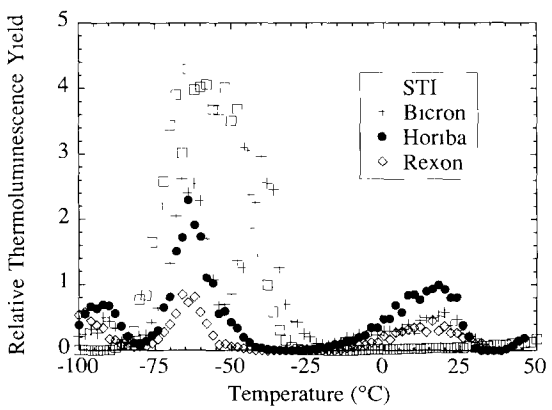

Fig. 8. CsI(Tl) thermoluminescence "glow curves," for crystals from Bicron Corp., Horiba Crystal Products, Rexon Components, Inc., and Solon Technologies, Inc. measured by current mode method.

observed that all of the crystals have thermoluminescence emission peaks at about −65°C, the STI crystal either has peaks at −65 and −55°C or one very broad peak, the Bicron, Horiba, and Rexon crystals have peaks at about −90 and +20°C, and the Bicron crystal has an additional peak at about −40°C. We do not know why these significant crystal-to-crystal differences are observed, but using CsI(Tl) crystals in temperature ranges of large thermoluminescence yield may lead to erroneous results.

The thermal equilibrium release of thermoluminescence also affects other measurements. As previously mentioned, the relative peak count rate in emission spectrum measurements will probably be erroneous in temperature ranges of large thermoluminescence yield. However, thermoluminescence was not observed to change the shape of the emission spectrum. In luminescence timing spectra, the thermoluminescence manifests itself as an increase in the chance coincidence rate. Although this should not affect the modified Bollinger–Thomas results, it further obscures the long decay time constant by decreasing the signal-to-noise. Similarly, the presence of thermoluminescence will decrease signal-to-noise for other pulse mode methods.

7. Discussion

The emission spectrum and decay time constants of CsI(Tl) have been measured over the temperature range of −100 to +50°C. Emission spectra observed at room temperature in crystals from different vendors showed negligible differences. The decay times for the four different crystals were found to vary by less than 10% at 0°C and by 17% at room temperature. The relative scintillation yield and thermoluminescence "glow curves" were also measured in the same temperature range. Crystals from different vendors were observed to have similar scintillation yield temperature dependence, with yields peaking at temperatures ranging from −30 to −20°C. Thermoluminescence emissions were found to peak at about −65°C for all crystals, while peaks at −90, −40, +20, and possibly −55°C were observed for some crystals. For the STI crystal, it was found that thermoluminescence in the range of −80 to −30°C affects both current and pulse mode measurements because of small temperature oscillations and/or temperature gradients across the crystal. Similar problems should arise for any CsI(Tl) crystal in temperature ranges of large thermoluminescence yield. An important implication of these thermoluminescence findings is that results of applications that require room temperature operation in current mode could be susceptible to temperature fluctuations.

The two primary decay time constants, τ_1 and τ_2, were found to increase approximately exponentially

Table 5
Expected wavelength-averaged quantum efficiencies for a typical silicon PIN photodiode coupled to CsI(Tl) and expected absolute scintillation yield of CsI(Tl)

Temperature [°C]	Internal quantum efficiency	External quantum efficiency	Absolute scintillation yield [a] [photons/MeV]
+50	0.896	0.685	60100
+25	0.897	0.687	64800
0	0.898	0.689	66800
−25	0.900	0.691	68200
−50	0.902	0.694	62500
−75	0.907	0.702	55200
−100	0.912	0.709	40400

[a] Based on a room temperature absolute scintillation yield of 64800 photons/MeV [1] and relative scintillation yield results.

with inverse temperature. A significant rise time constant was found to populate τ_1 and increases exponentially with inverse temperature as well. The SSW method was found to reach its limits of applicability due to the length of τ_2 at about −60°C. The modified Bollinger–Thomas method was found to have problems in accurately determining τ_2 because of poor signal-to-noise. The signal-to-noise became worse with decreasing temperature due to the increasing decay times and could have been further degraded by thermoluminescence light.

Although the emission spectrum measurements for the STI crystal probably included thermoluminescence light in the −80 to −30°C range, it was not observed to affect the shape of the spectrum. With the emission spectrum shape known, the expected quantum efficiency for a given photodetector can be calculated. Table 5 shows the expected internal and external wavelength-averaged quantum efficiencies for CsI(Tl) when coupled to a typical silicon PIN photodiode along with the expected absolute scintillation yield of CsI(Tl). The wavelength-averaged quantum efficiencies increase with decreasing temperature because of the decreasing amount of light emitted at short wavelengths.

An ultra-fast decay component was also confirmed. Our best estimate of the decay time is < 0.5 ns, but it has been previously reported to be < 10 ps by Deich et al. [19,20]. The yield of the ultra-fast component appears to be independent of temperature and accounts for roughly 0.2% (about 100 photons/MeV for gamma rays) of the total light yield for the PMT used. This yield is too small to be seen in our emission spectrum measurements, but has been reported to have a broad emission band that peaks around 620 nm [19]. The ultra-fast component is of limited use in gamma-ray experiments because of this long wavelength of emission. The quantum efficiency of typical photocathodes at 620 nm is very low, such that a typical yield will be < 1 photoelectron/MeV. Although the quantum efficiency of photodiodes is typically very good at 620 nm, the photodiode noise will tend to obscure this small signal.

The scintillation yield peaks at about −30°C for the STI crystal. The decrease in scintillation yield below the peak is at least partially due to energy being stored in the crystal. This stored energy is the source of the thermoluminescence light that is released when the crystal is warmed. The peaking of the scintillation yield at −30°C suggests that energy resolution of CsI(Tl) should be optimized at this temperature. However, the long decay time is on the order of the longest commercially-available amplifier shaping time, resulting in a significant ballistic deficit. In fact, the ballistic deficit causes the amplifier output pulse amplitude (or photopeak centroid) to decrease with temperature below about +10°C independent of amplifier shaping time, even though the scintillation yield is increasing down to −30°C. Improving the energy resolution of CsI(Tl)/photodiode detectors below room temperature is thus not as promising as originally hoped. Since the scintillation yield variations with temperature are relatively small, other factors, such as decay times and thermoluminescence, will dictate the optimum operating temperature.

Acknowledgements

We would like to thank Ruvin Deich for his helpful discussions, Tim DeVol for his assistance in performing measurements to confirm the experimental results, and Valentin Jordanov for his assistance with the shaped square wave method. The research was performed while J. Valentine was under appointment to the Nuclear Engineering and Health Physics Fellowship Program administered by Oak Ridge Associated Universities for the US Department of Energy. W. Moses would like to thank the Whitaker Foundation for support. This work was supported in part by the US Department of Energy under contracts No. DE-AC03-76SF00098 and No. DE-FG02-86NE37969, in part by the National Heart, Lung, and Blood Institute, National Institute of Health, and National Cancer Institute under grants No. P01-HL25840 and No. R01-CA48002.

References

[1] J.D. Valentine, D.K. Wehe, G.F Knoll and C.E. Moss, Conf. Record 1991 IEEE Nucl. Sci. Symp. 1 (1991) p. 176, submitted to IEEE Trans. Nucl. Sci.

[2] J. Geist, W.K. Gladden and E.F. Zalewski, J. Opt. Soc. Am. 72 (1982) 1068.
[3] I.K. Pliavin', Opt. Spectrosc. VII (1) (1959) 41.
[4] N P. Sastry and B.V. Thosar, Proc. Ind. Acad. Sci. 54A (1961) 140.
[5] W.W. Managan, IRE Trans. Nucl. Sci. NS-9 (1962) 1.
[6] S. Masunaga, I. Morita and M. Ishiguro, J. Phys. Soc. Jpn 21 (1966) 638.
[7] P. Schotanus, R. Kamermans and P. Dorenbos, IEEE Trans. Nucl. Sci. NS-37 (1990) 177.
[8] P. Kreutz, A Kuhmichel, C. Pinkenburg and J. Pochodzalla, Nucl. Instr. and Meth. A260 (1987) 120
[9] H. Grassmann, E. Lorenz and H.G. Moser, Nucl. Instr. and Meth. 228 (1985) 323.
[10] R.G. Lagu and B.V. Thosar, Proc. Ind. Acad. Sci. 53A (1961) 219
[11] B.C. Grabmaier, IEEE Trans. Nucl. Sci. NS-31 (1984) 372.
[12] V B. Gutan, L.M. Shamovskii, A.A. Dunina and B.S. Gorobets, Opt. Spectrosc. 37 (1974) 407.
[13] R. Gwin and R.B. Murray, Phys. Rev. 131 (1963) 508.
[14] T. Towyama, I. Morita and M. Ishiguro, J. Phys. Soc. Jpn 25 (1968) 1133.
[15] C.J. Crannell, R.J. Kurz and W. Viehmann, Nucl. Instr. and Meth. 115 (1974) 253.
[16] L.M. Bollinger and G.E. Thomas, Rev. Sci. Instr. 32 (1961) 1044.
[17] M. Moszynski and B. Bengtson, Nucl. Instr. and Meth. 142 (1977) 417.
[18] J.D. Valentine, V.T. Jordanov, D.K. Wehe and G.F. Knoll, Nucl. Instr. and Meth. A314 (1992) 119.
[19] R.G. Deich, M. Karklina and L. Nagli, Solid State Commun. 71 (1989) 859.
[20] E.D. Aluker, V.V. Gavrilov, R.G. Deich and S.A. Chernov, JETP Lett. 47 (1988) 142.
[21] J.B. Birks, The Theory and Practice of Scintillation Counting (Pergamon Press, Oxford, 1964).
[22] J. Pellaux, Helv. Phys. Acta 49 (1976) 700.